Available online at www.sciencedirect.com
SCIENCE DIRECT
Thin Solid Films 490 (2005) 101 – 107
thin solid films
www.elsevier.com/locate/tsf

Microstructure and photoelectrochemical characterization of the TiO_2–SnO_2 system

K. Zakrzewska[a,*], M. Radecka[a], J. Przewoźnik[a], K. Kowalski[a], P. Czuba[b]

[a] AGH-University of Science and Technology, 30-059 Kraków, al. Mickiewicza 30, Poland
[b] Institute of Physics, Jagiellonian University, 30-059 Kraków, ul. Reymonta 4, Poland

Available online 4 June 2005

Abstract

The isostructural system of TiO_2–SnO_2 has recently emerged as a promising candidate for gas detection. Thin films of TiO_2–SnO_2 have been deposited onto different substrates at 620 K by the rf sputtering from a Ti–SnO_2 target. In order to cover a full compositional range from 100% TiO_2 to 100% SnO_2 in the film, the target surface ratio of SnO_2/Ti has been varied. The crystallographic structure and film morphology have been investigated by means of GID and AFM. The oxidation states of tin and titanium ions have been studied by the Mössbauer spectroscopy combined with XPS. From the photoelectrochemical kinetics, longer relaxation times have been found for TiO_2–SnO_2 than those for pure TiO_2. The electron trap levels are proposed to account for this observation.

Keywords: Oxides; Mössbauer spec.; Photoconductivity; X-ray photoelectron spectroscopy (XPS)

1. Introduction

Since the first report of Chung et al. in 1992 on the application of TiO_2–SnO_2 as a stable CH_4 and CO sensor [1], this mixed oxide system has become a very promising candidate for gas detection purposes. The improved gas sensing performance was attributed to the Schottky barrier formation at the boundaries of well-developed SnO_2 grains finely dispersed in the TiO_2 amorphous matrix. Later, a systematic study of the series of compounds $(Sn_{1-z}Sb_z)_{1-x}Ti_xO_2$ $(0 \leq x \leq 1,\ z = 0,\ 0.01,\ 0.05)$ was undertaken by Dusastre and Williams [2]. The model was proposed to account for the composition dependence of gas-sensitivity.

Our previous studies of the TiO_2–SnO_2 mixed oxide in the form of both thin films and polycrystalline ceramics [3–5] concentrated upon the influence of the chemical composition on the transport and optical properties, crystal structure and the sensitivity to the reducing gases such as hydrogen and methane. It was concluded [4] that (a) small additions of Ti in SnO_2 increased the density of centers active for the chemisorption, (b) degradation of the electrical properties upon prolonged thermal treatment, typical of SnO_2, did not occur in the case of TiO_2–SnO_2 sensors, (c) high operating temperatures of TiO_2 sensors could be reduced to about 770 K as a result of Sn incorporation.

It was realized relatively early [6,7] that a profound structural analogy between TiO_2 and SnO_2 could make the mixed oxide system of TiO_2–SnO_2 very interesting for applications as well as for the fundamental research. Both oxides belong to the same crystal symmetry (tetragonal) with the space group D_{4h}^{14} and two molecular units per primitive unit cell (see Table 1). They both crystallize within the rutile structure. Hence, they can easily form a solid solution. Because the TiO_2–SnO_2 is one of the best examples of spinodal decomposition in ceramic samples, the thermodynamic and crystallographic properties have been extensively studied [6–8]. It is well established now that above a critical temperature depending on the chemical composition, a solid solution of TiO_2–SnO_2 occurs over a full composition range while below the spinodal decomposition takes place. As expected, the lattice parameters (a, c)

* Corresponding author. Tel.: +48 12 617 2901; fax: +48 12 633 23 98.
E-mail address: zak@uci.agh.edu.pl (K. Zakrzewska).

0040-6090/$ - see front matter © 2005 Elsevier B.V. All rights reserved.
doi:10.1016/j.tsf.2005.04.035

Table 1
Comparison of the basic properties of SnO_2 and TiO_2

Physical property	SnO_2	TiO_2
Crystallographic structure	Rutile	Rutile
Symmetry	Tetragonal	Tetragonal
Metal coordination	Octahedral	Octahedral
Space group	$D_{4h}^{14} - P4_2/nmm$	$D_{4h}^{14} - P4_2/mnm$
Lattice parameters	$a=0.4738$ nm	$a=0.4594$ nm
	$c=0.3188$ nm	$c=0.2958$ nm
Density	6.994 – 7.02 g cm^{-3}	4.26 g cm^{-3}
Debye temperature	570 K	758 K
Melting point	>1400 K	2100 K
Band gap	3.6 eV	3.03 eV
Effective mass of electrons	0.3 m_e	30–50 m_e

of the system increase continuously from those of TiO_2 to those of SnO_2. The ionic radius of Sn^{4+} (0.071 nm) being larger than that of Ti^{4+} (0.068 nm) accounts for the observed lattice expansion. However, the linear relationship between the chemical composition and the lattice constant, known as a Vegard rule, is not always obeyed [8].

As far as the electronic structure is concerned the similarities between TiO_2 and SnO_2 end (Table 1). The differences concern the band gap energies and the character of valence band-conduction band transitions (direct, indirect) as well as the effective mass of electrons related to the shape of the conduction band.

Little is known about the electronic structure of TiO_2–SnO_2. Much more profound understanding of the electronic structure of TiO_2–SnO_2 system seems to be necessary for designing gas sensors with the optimized composition. Spectrophotometric measurements reveal [9] that the band gap of TiO_2–SnO_2 system increases systematically with the increasing SnO_2 concentration from about 3.3 eV (TiO_2) to 3.8 eV (SnO_2). Recently, the theoretical calculations using a cluster model have been performed by Sensato et al. [10], on the basis of which they could establish the evolution of the fundamental parameters (band gap, Fermi level, etc.) of the electronic structure of TiO_2–SnO_2.

Many problems still need to be resolved because they have not yet been investigated in depth. One of them is the evolution of the oxidation states of Ti and Sn ions entering the structure of TiO_2–SnO_2. It is often taken for granted, without any special experimental evidence, that Ti and Sn ions are isovalent when substituting for each other in the solid solution. The generally assumed oxidation degree is +4. The mechanism of gas sensing involves, in the first step, the chemisorption of oxygen species O^-, O^{2-} or O_2^- at the adsorption sites. The presence of Sn^{2+}, Ti^{3+} or Ti^{2+} ions, with different that Sn^{4+} (typical for SnO_2) and Ti^{4+} (typical for TiO_2) oxidation states, may affect this interaction and subsequently the sensors performance. The lack of the systematic experimental studies of this kind has been a motivation for the current work on the oxidation states of Ti and Sn and the electronic structure of TiO_2–SnO_2. The aim of this paper is to resolve this issue by means of XPS and Mössbauer spectroscopies. The photoelectrochemical experiment concerning dynamic responses of the system to light has been proposed as a complementary method in the studies of the relaxation processes.

2. Experimental

Thin films of TiO_2–SnO_2 were deposited onto different substrates (amorphous silica, Ti foil) at 620 K by the rf sputtering from a Ti–SnO_2 target. In order to cover a full compositional range from 100% TiO_2 to 100% SnO_2 in the film, the target surface ratio of SnO_2/Ti was varied. The parameter Θ_{SnO_2} defined as the area covered with SnO_2 to the area of Ti target was introduced. Large differences in the melting points of titanium (1940 K) and tin (500 K) as well as quite different sputtering yields of these two metals in the oxygen atmosphere are the basic technological constrains as far as the deposition of (Ti,Sn)O_2 thin films is considered. Oxygen adsorption on the surface of Ti target reduces considerably its sputtering yield. Low melting temperature of tin requires special bonding of the metallic tin to the Ti target. Therefore, a special target has been designed. It consists of tin, well bonded to the baseplate to provide good thermal contact, covered by a Ti disc with circular openings. By covering a certain number of these openings by Ti foil, one can change in fairly easy, reproducible manner the area percentage of the target coverage and the film composition.

For deposition of films with TiO_2-rich compositions, the sputtering of the dielectric target has been chosen. Higher melting point of SnO_2 than that of Sn allows using Ti metallic target covered with SnO_2 tablets.

The chemical composition of the films was determined by means of the Electron Microprobe (EMP) and X-ray Photoelectron Spectroscopy (XPS). XPS combined with Mössbauer spectroscopy was used to study the oxidation states of Ti and Sn ions.

X-ray photoelectron spectra were recorded using a VSW Scientific Instruments electron spectrometer equipped with a MgK_α (1253.6 eV) anode as a source of X-ray radiation. The binding energy shifts due to the surface charging have been corrected assuming the C 1s XPS peak at 284.6 eV. The depth of the XPS analysis is limited to about 6 nm.

The ^{119}Sn Mössbauer effect measurements were performed in the transmission geometry using a constant acceleration type spectrometer, $Ba^{119}SnO_3$ as the source and the NaJ/Tl scintillation counter. The Mössbauer spectra were fitted using a transmission integral in order to take into account the absorber thickness effects. The spectra were refined with quadrupole doublets of Lorentzian lines assuming a nonzero value of the electric field gradient at the tin site. Hyperfine parameters, the isomer shift δ_{IS} and quadrupole splitting Δ_{QS} were found. The values of isomer shift are given relative to the $Ba^{119}SnO_3$ source kept at room temperature RT.

After fitting the Mössbauer spectrum, the corrected subspectral areas corresponding to Sn^{4+} (S_{SnO_2}) and Sn^{2+} (S_{SnO}) were calculated. From the corrected subspectral areas

S_{SnO_2}, S_{SnO} and the recoil-free fractions f_{SnO_2}, f_{SnO} the relative molar contribution γ defined as

$$\gamma = \frac{Sn^{2+}}{Sn^{4+}} = \frac{f_{SnO_2}}{f_{SnO}} \frac{S_{SnO}}{S_{SnO_2}} \quad (1)$$

was determined.

The crystallographic studies were carried out by means of X-ray diffraction in grazing incidence (GID) configuration with X'Pert MPD Philips diffractometer. Atomic force microscopy AFM (SPM Park Sci. Instr.) in the contact mode was used to determine the film microstructure.

Photoelectrochemical characterization of the relaxation processes at a semiconductor/electrolyte interface relies on the photocurrent transients, i.e., I_{ph} vs. time measurements in the electrochemical cell with the Ti anode overcoated with a thin layer of TiO_2–SnO_2 [11]. The photoelectrochemical experiments were performed in a standard cell consisting of a photoanode, a working electrode and a reference electrode (SCE) with a TRIAX 180 Jobin Yvon monochromator and a 450-W Xe lamp as a light source. The electrodes were immersed in a buffer solution with pH=8.

The photocurrent responses to the white light were recorded with a Keithley 6517A electrometer and a manually operated light chopper at 0 V bias.

3. Results and discussion

From our previous studies [3–5] it could be inferred that the conditions of nucleation and growth of SnO_2 thin films are different from those of TiO_2. The SnO_2 and SnO_2-rich films crystallize in the rutile structure even at room temperature. On the contrary, TiO_2-rich compositions are usually amorphous and in order to crystallize an additional energy transfer to growing film is required. Fig. 1 shows X-ray diffraction patterns of a series of TiO_2–SnO_2 thin films with the varying tin atomic content defined as $x=Sn/(Sn+Ti)$. When the substrate temperature is fixed at 620 K, TiO_2 crystallizes as anatase but even a small addition of Sn changes the crystallographic structure to that of tetragonal rutile. X-ray diffraction peaks are shifted from the positions characteristic to TiO_2-rutile due to the change in the lattice parameters upon the substitution of Sn for Ti. With the increasing tin content, X-ray diffraction lines shift systematically towards positions typical for tetragonal, cassiterite form of SnO_2. Apparently, no other phases are observed in GID patterns. As the growing conditions of thin films are far from equilibrium, it seems possible to observe solid solutions over the compositional range where normally one would expect decomposition to take place.

Fig. 2 presents the AFM morphological images of TiO_2–SnO_2 thin films. In order to reveal the possible precipitation of grains with different mechanical properties, a special mode of operation of AFM, Lateral Force Microscopy

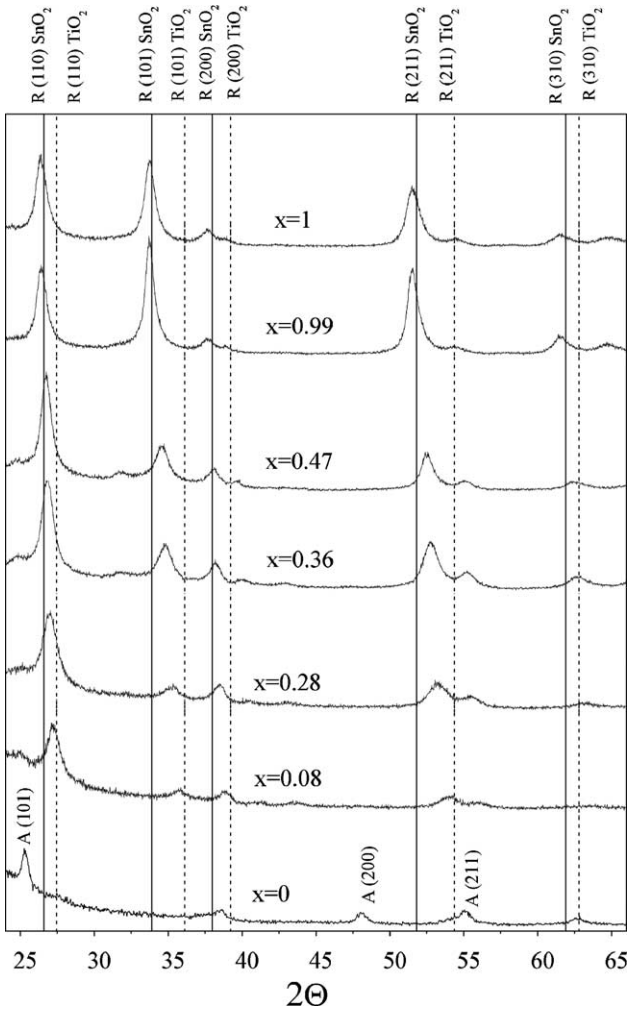

Fig. 1. X-ray diffraction patterns at grazing incidence GID for TiO_2–SnO_2 thin films deposited by reactive rf sputtering. Varying chemical composition is reflected by the changes in $x=Sn/(Sn+Ti)$. A—denotes anatase, R—rutile. Solid lines represent JCPDS standard for rutile SnO_2 (cassiterite) while dashed lines correspond to rutile TiO_2.

(LFM) was used. As shown in Fig. 2, the microstructure of thin films obtained by reactive rf sputtering is much more affected by the thermal treatment than by the incorporation of Sn. Small anatase grains are obtained when TiO_2 thin film is grown at 620 K (Fig. 2a). At 970 K TiO_2 is already transformed to rutile and large grains can be observed for pure TiO_2 (Fig. 2b) and for TiO_2–SnO_2 thin films (Fig. 2c). The comparison between AFM (Fig. 2c) and LFM (Fig. 2d) for the same TiO_2–SnO_2 sample ($x=0.43$) gives no evidence concerning the possible precipitation of different phases. Grains appear to be more or less homogeneously distributed laterally.

The objective of the XPS studies in TiO_2–SnO_2 system is twofold. Primarily, it is of great interest to establish the oxidation states of Ti and Sn ions from the analysis of binding energies of photoelectrons. Not only Ti^{4+} related to TiO_2 but also lower oxidation states Ti^{2+} and Ti^{3+} have been reported [5,12,13]. The presence of Sn^{2+} is difficult to

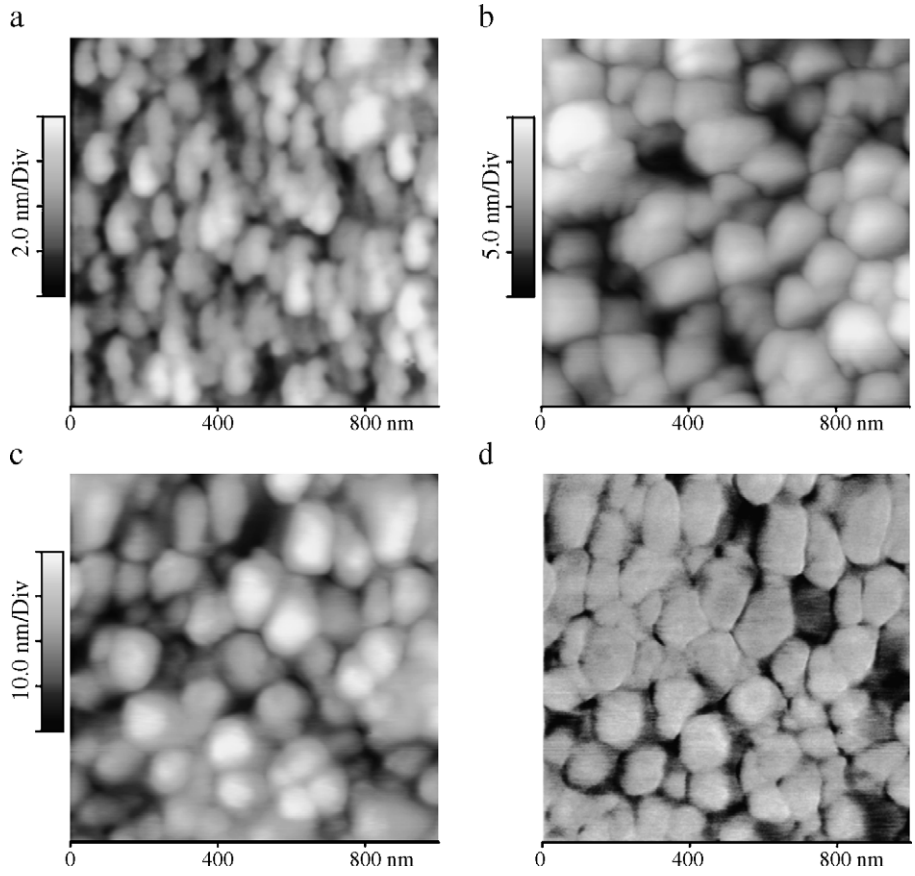

Fig. 2. Atomic force microscopy (AFM) and lateral force microscopy (LFM) images for thin films deposited by reactive sputtering: (a) TiO_2, substrate temperature of 620 K (AFM), (b) TiO_2 annealed at 970 K (AFM), (c) TiO_2–SnO_2 with $x=0.43$, annealed at 970 K (AFM), (d) TiO_2–SnO_2 with $x=0.43$, annealed at 970 K (LFM).

establish on the basis of XPS alone because the binding energies of electrons corresponding to the Sn^{4+} and Sn^{2+} ions are close to each other (less than 0.7 eV separation) and the spectral lines overlap [14]. Hence, the contributions from these states are difficult to distinguish in the XPS spectrum. Therefore, Mössbauer spectroscopy was used as a complementary technique.

The second objective of the XPS investigations in TiO_2–SnO_2 system is to establish the relative ratio of $x=Sn/(Sn+Ti)$ as a function of the technological parameters such as the target surface coverage with SnO_2. Quantitative analysis of XPS spectra, preceded by deconvolution and fitting of the relevant peaks, is based on the fact that the peak area is proportional to the atomic concentration of the corresponding elements. The proportionality constant contains the relative sensitivity factor that is determined by the photoionization process and conditions of experiment. In our case these factors were found to be: 1 for C 1s by definition, 13.48 for Sn $3d_{5/2}$ and 4.95 for Ti $2p_{3/2}$.

The summary of XPS results is presented in Table 2. As shown in Table 2, the binding energies of Ti $2p_{3/2}$ and Sn $3d_{5/2}$ remain unaffected by the varying chemical composition of TiO_2–SnO_2 system. The Ti $2p_{3/2}$ peak position in TiO_2–SnO_2 is comparable to that observed for undoped TiO_2 (458.6 eV). Therefore, one can conclude that titanium is present as Ti^{4+}. In fact, the Ti $2p_{3/2}$ peak consists of two contributions: the major one (of about 96–97%) at about 458.6 eV attributed to Ti^{4+} and a much less significant (3–4%) at about 455.1–456.3 eV representing lower oxidation

Table 2
Summary of XPS studies for TiO_2–SnO_2 thin films

Θ_{SnO_2}	x=Sn/(Sn+Ti)		BE (eV)		
	EMP	XPS	Sn $3d_{5/2}$	Ti $2p_{3/2}$	O 1s
1	1	1	486.4	–	530.2
					532.3
0.993	0.995	0.993	486.4	458.8	530.4
					532.3
0.980	0.99	0.989	486.3	458.5	530.2
					531.9
0.074	0.47	0.607	486.2	455.5	529.9
				458.4	532.1
0.053	0.36	0.529	486.4	455.5	530.0
				458.6	532.0
0.032	0.28	0.414	486.1	455.2	529.7
				458.4	531.7
0.011	0.08	0.10	486.1	455.1	529.8
				458.5	532.5
0	0	0	–	456.3	530.0
				458.6	531.9

Binding energies (BE) of Sn $3d_{5/2}$, Ti $2p_{3/2}$ and O 1s are corrected for C 1s at 284.6 eV.

states Ti^{3+} or Ti^{2+}. Therefore, a small contribution from lower oxidation states cannot be completely ruled out (Table 2).

The comparative analysis of Sn $3d_{5/2}$ peak position in SnO_2 and TiO_2–SnO_2 indicates that the binding energy is the same and may be attributed to the Sn^{4+}. On the basis of XPS results, the presence of metallic Sn^0 can be excluded because its BE is shifted by about 2.2 eV from the Sn^{4+}.

The quantitative analysis suggests that for x close to 0 or 1, the results of the X-ray Electron microprobe and XPS remain in good agreement. This is not the case for the intermediate compositions ($0.2 < x < 0.6$). Over this range, in the ceramic samples, the decomposition takes place. Here, the value of x determined from XPS is always larger than that from EPS. As XPS gives the information from the film surface while EPS probes the bulk of the sample, one can only conclude that the excess of tin is accumulated at the surface. The inhomogeneous distribution of Sn in depth has been confirmed by SIMS.

The representative Mössbauer spectra of TiO_2–SnO_2 thin films are shown in Fig. 3a–c. Reference spectra of the SnO_2 powders intentionally mixed with the known molar concentration of SnO are given for comparison (Fig. 3d,e). For the powder samples, lines characteristic of Sn^{2+} (SnO) and Sn^{4+} (SnO_2) are observed. The measured hyperfine parameters of SnO (δ_{IS}=2.599±0.002 mm/s and Δ_{QS}= 1.318±0.002 mm/s) and those of SnO_2 (δ_{IS}=−0.025± 0.001 mm/s and Δ_{QS}=0.498±0.002 mm/s) at RT are in agreement with the usually accepted ones for these compounds [15–17]. In the case of thin films of SnO_2–TiO_2 obtained by rf reactive sputtering, the absence of any but one signal at δ_{IS}=0.038±0.005 mm/s with Δ_{QS}= 0.566±0.006 mm/s was noted. This signal arises from Sn^{4+} oxidation state. Both the isomer shift and quadrupole splitting remain almost unaffected by the change in TiO_2–SnO_2 composition. This is in concordance with the formation of a solid solution. The oxidation state corresponding to Sn^{2+} is detected in SnO_2 thin films obtained by RGTO (Rheotaxial Growth and Thermal Oxidation) technique, only (Fig. 3c).

In order to verify the possibility of Sn^{2+} oxidation state in TiO_2–SnO_2 thin films prepared by rf reactive sputtering, the comparative studies have been carried out. In order to perform the quantitative analysis and determine the relative molar contribution $\gamma=(Sn^{2+})/(Sn^{4+})$ in thin films, the recoil-free fraction should be known. However, due to the discrepancies in the values reported in the literature [15,16,18], we have adopted the following procedure. From

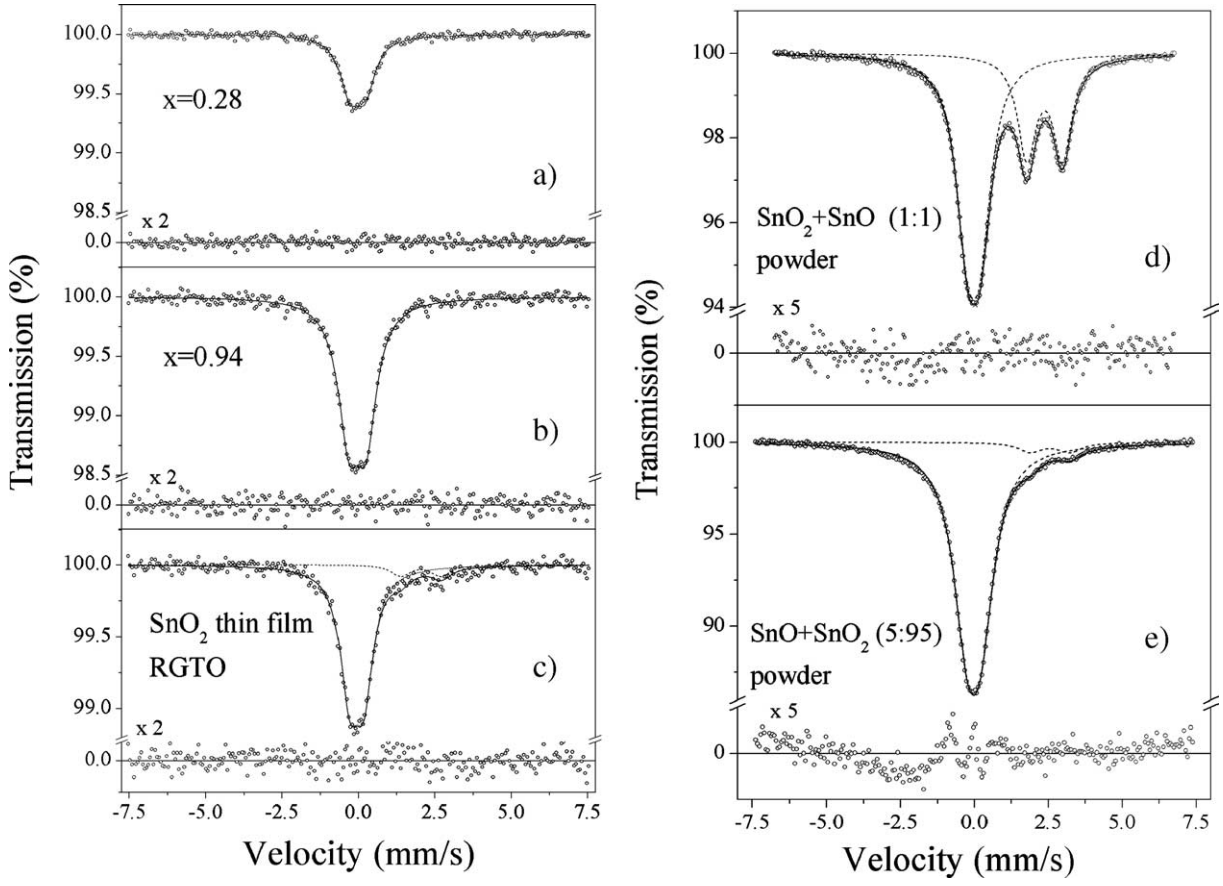

Fig. 3. Mössbauer transmission spectra of (a) TiO_2–SnO_2 thin film with x=0.28 deposited by reactive sputtering, (b) TiO_2–SnO_2 thin film with x=0.94 deposited by reactive sputtering, (c) SnO_2 thin film prepared by RGTO method, (d) SnO and SnO_2 powder mixed with the molar ratio 1:1, (e) SnO and SnO_2 powder mixed with the molar ratio 5:95.

the reference spectrum in Fig. 3d and Eq. (1), the ratio of the recoil-free fraction $(f_{SnO_2})/(f_{SnO})$ was found to be of about 1.818. In was further assumed that this value remains the same for thin films (Fig. 3c) and powders with different molar concentrations (Fig. 3e). For the mixture of the SnO and SnO_2 powders with the molar ratio 5:95 (Fig. 3e), one can see that such a small contribution of SnO to SnO_2 spectrum is clearly detectable from the Mössbauer spectrum. The value of $\gamma = 0.093 \pm 0.007$ as determined from Eq. (1) is larger than nominal 0.053. This large difference is most probably due to the broadening and non-Lorentzian shape of the SnO_2 lines. This result could be improved by using more elaborate models of fitting. Therefore, one should realize that this method shows strong tendency towards overestimation of SnO phase contribution when admixed in small quantity.

The same method of analysis was applied to the Mössbauer spectrum measured for SnO_2 thin film prepared by RGTO method (Fig. 3c) and $\gamma = 0.174 \pm 0.017$ was found. The Mössbauer spectra for thin films deposited by reactive sputtering clearly do not show any detectable amounts of Sn^{2+} ions. The spectra were satisfactory fitted by a single quadrupole doublet corresponding to SnO_2 phase.

Dynamic responses of the system to light give us information concerning the mechanism of electron–hole relaxation and allow us to draw conclusions regarding the electronic structure of TiO_2–SnO_2. Combined with the optical characterization by the spectrophotometric measurements, the XPS data and the results of the microstructural studies, this technique is a valuable tool in the interpretation of processes involved in the TiO_2–SnO_2 system.

Photocurrent transients, i.e., shape of the photocurrent response to the switch on and off of the illumination, rise and decay times of the signal, depend on the photogeneration of charge carriers (electron and holes) and the relaxation mechanism. Under uv excitation, the electrons are excited from the valence band to the conduction band of a semiconductor such as TiO_2 or SnO_2. This process leaves the holes behind. In the electric field, the photogenerated holes are separated from the photoelectrons. Holes move to the semiconductor surface, where they are trapped or captured by reduced species in the electrolyte, while the electrons are transported to the back contact of the electrode.

Fig. 4 shows two different types of photocurrent responses. In the case of TiO_2 the initial increase in I_{ph} is followed by an exponential decrease with time. This initial maximum (anodic spike) is caused by a separation of the photogenerated electron–hole pairs at the semiconductor/electrolyte interface [19]. The photocurrent decay indicates that recombination processes are occurring. Holes reaching the semiconductor surface may, instead of capturing electrons from the electrolyte accumulate at the surface and recombine with electrons from the conduction band, i.e., the decay is determined by the rate at which minority carriers trapped at the surface states capture majority

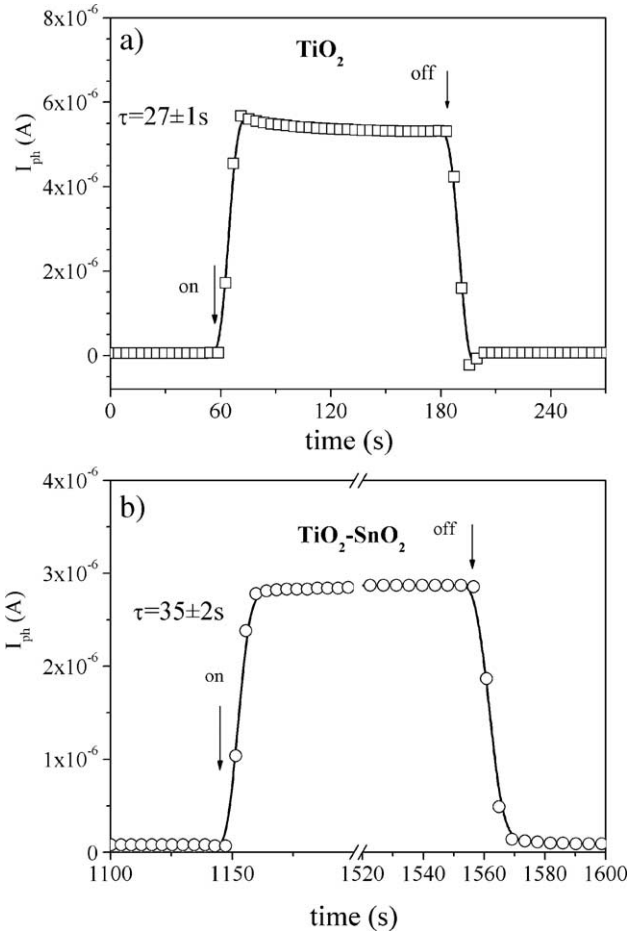

Fig. 4. Transient photocurrent I_{ph} response of (a) TiO_2, (b) TiO_2–SnO_2 ($x = 0.08$) thin film electrodes in an electrolyte of pH = 7 under illumination with white light at 0 V vs. SCE. Arrows indicate when light was turned on and off.

carriers. Another recombination process giving rise to a decay of the photocurrent relies on the fact that conduction band electrons start to reduce the photogenerated oxidized species in the electrolyte. When the light is switched off, a cathodic spike is observed due to the back reaction of conduction band electrons with holes trapped at the surface. The transient time constant τ, defined in [20], was found to be 27 ± 1 s.

However, when the TiO_2 film contains tin (Fig. 4b) the spikes are no longer seen and the transient time constant is higher and amounts to 35 ± 2 s. In order to account for this it is assumed that the increased energy of the Fermi level [10] and the existence of trap levels are responsible for this effect. The electrons trapped in the surface states may act as recombination sites for the photogenerated holes causing an increase in the rise time of the photocurrent.

4. Conclusions

Systematic, experimental studies of the TiO_2–SnO_2 mixed oxide thin films have been performed within a full

compositional range from 100% TiO_2 to 100% SnO_2 with the ultimate aim to gain a deeper understanding of the gas sensing properties of the system. The following conclusions could be drawn:

- Incorporation of tin into TiO_2 stabilizes the rutile crystallographic phase.
- Contrary to the case of ceramic samples, solid solutions are formed over the full compositional range in the case of thin films deposited by rf sputtering at 620 K.
- Combined techniques of XPS and Mössbauer spectroscopy reveal Sn^{4+} and Ti^{4+} as the predominant ions in the system.
- Comparison between EMP and XPS suggests that the excess of Sn is accommodated at the film surface. SIMS results confirm this conclusion.
- The photocurrent transients have different character for TiO_2-SnO_2 and TiO_2 thin films. Incorporation of tin results in the formation of electron trap levels not present in the case of pure TiO_2.

Acknowledgement

One of the authors (K. Zakrzewska) is grateful for the financial support under the project No. 11.11.120.068.

References

[1] W.Y. Chung, D.D. Lee, B.K. Sohn, Thin Solid Films 221 (1992) 304.
[2] V. Dusastre, D.E. Williams, J. Mater. Chem. 9 (1999) 445.
[3] M. Radecka, K. Zakrzewska, M. Rękas, Sens. Actuators, B, Chem. 47 (1998) 194.
[4] K. Zakrzewska, Thin Solid Films 391 (2001) 229.
[5] K. Zakrzewska, M. Radecka, M. Rękas, Thin Solid Films 310 (1997) 161.
[6] V.S. Stubican, A.H. Schultz, J. Am. Ceram. Soc. 5 (1968) 290.
[7] D. Garcia, D. Speidel, J. Am. Ceram. Soc. 55 (1972) 322.
[8] M.W. Park, T.E. Mitchell, A.H. Heuer, J. Am. Ceram. Soc. 58 (1975) 43.
[9] M. Radecka, P. Pasierb, K. Zakrzewska, M. Rękas, Solid State Ionics 119 (1999) 43.
[10] F.R. Sensato, R. Custodio, E. Longo, A. Beltrán, J. Andrés, Catal. Today 85 (2003) 145.
[11] M. Radecka, Thin Solid Films 451–452 (2004) 98.
[12] A.F. Carley, P.R. Chalker, J.C. Riviere, M.W. Roberts, J. Chem. Soc., Faraday Trans. I 83 (1987) 351.
[13] E. McCafferty, J.P. Wightman, Appl. Surf. Sci. 143 (1999) 92.
[14] J. Szuber, G. Czempik, R. Larciprete, D. Koziej, B. Adamowicz, Thin Solid Films 391 (2001) 198.
[15] R.H. Herber, Phys. Rev., B 27 (1983) 4013.
[16] M.S. Moreno, R.C. Mercader, Phys. Rev., B 50 (1994) 9875.
[17] G.C. Collins, T. Kachnowski, N. Benczer-Koller, M. Pasternak, Phys. Rev., B 19 (1999) 1369.
[18] M.S. Moreno, R.C. Mercader, Hyperfine Interact. 83 (1994) 415.
[19] A. Hagfeldt, H. Lindström, S. Södergren, S.-E. Lindquist, J. Electroanal. Chem. 381 (1995) 39.
[20] D. Tafalla, P. Salvador, R.M. Benito, J. Electrochem. Soc. 137 (1990) 1810.